

# Self-Pulsed Electron Transmission through a Finite Waveguide in a Transversal Magnetic Field

Manamohan Prusty and Holger Schanz\*

Max-Planck-Institut für Dynamik und Selbstorganisation, und Fakultät für Physik, Universität Göttingen,  
Bunsenstr. 10, D-37073 Göttingen, Germany

(Received 29 October 2006; published 25 April 2007)

The distribution of scattering delay times is analyzed for classical electrons which are transmitted through a clean channel. For a nonzero magnetic field the distribution shows a regular pattern of maxima (logarithmic singularities). Although their location follows from a simple commensurability condition, there is no straightforward geometric explanation of this self-pulsing effect. Rather it can be understood as a time-dependent analog of transverse magnetic focusing, in terms of the stationary points of the delay time. We explain that this is a generic mechanism which may lead to singular delay distributions also in other scattering systems without commensurability effects.

DOI: 10.1103/PhysRevLett.98.176804

PACS numbers: 73.23.-b, 05.60.-k, 73.43.Cd

Ballistic semiconductor nanostructures offer fascinating opportunities to observe effects from the theory of classical dynamical systems. Recent experiments with confined two-dimensional electron gases (2DEG) revealed traces of chaos, nonlinear resonances, unstable periodic orbits or Kolmogorov-Arnold-Moser hierarchies in phase space [1], and also a variety of magnetic commensurability effects [2–4]. Among the latter, magnetic focusing [2] is of particular importance and has found numerous applications such as the detection of composite fermions [5] or the separation of spin states [6]. All these results were based on conductance measurements. However, it is well known that the transition probabilities alone provide only an incomplete description of a scattering system. Important additional information is contained, for example, in the delay time, i.e., the time spent by the scattered particle in the interaction region. In a seminal work Wigner had pointed out the equivalence between the delay time and the energy derivative of the phase of transition amplitudes [7]. Ever since there has been a lot of theoretical and experimental activity devoted to understanding the distribution of this quantity in various physical contexts [8], including, in particular, also mesoscopic transport through systems with nonlinear dynamics [9–12]. For semiconductor nanostructures there exist pioneering measurements of picosecond delays for ballistic electrons in a magnetic focusing geometry [13]. Moreover, experimental access to the scattering phase (e.g., in quantum dots [14]) might result in an electronic implementation of Wigner's relation in the near future.

Here we analyze the delay-time distribution for the transmission of electrons through a clean channel with a transversal magnetic field [Fig. 1(a)]. This model is utterly simple but not unrealistic in the above context. It can be realized as a finite constriction in a 2DEG, and the delay distribution may be obtained, e.g., from the time-resolved current response to a picosecond voltage pulse similar to [13]. We predict a rather surprising self-pulsing effect: a number of electrons entering the interaction region at the

same moment of time exit from the channel bunched together in packets which form a nearly periodic train. Specifically we calculated numerically the distribution of trajectory lengths from entry to exit and obtained a histo-

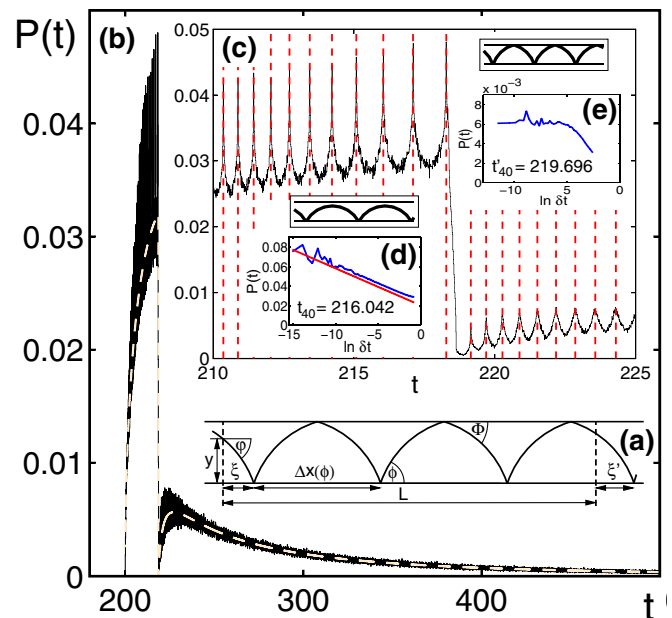


FIG. 1 (color online). (a) A typical electron trajectory transmitting through a channel of length  $L$  under the influence of a perpendicular magnetic field. (b) Distribution of transmission delays for  $r = 4$  and  $L = 200$ . The white dashed line is the average density, Eq. (7). The inset (c) magnifies the region around  $t^* \approx 218.5$  [Eq. (10)]. Here the dashed vertical lines mark the delay times  $t_n$  of orbits which are commensurate with the channel length (see text). The small insets demonstrate with two examples that the maxima  $t_n < t^*$  (d) actually are logarithmic singularities while this is not the case for  $t_n > t^*$  (e). In these semilogarithmic plots the density is shown as a function of  $\delta t = t - t_n$ . The straight line in (d) has the slope given in Eq. (25).

gram which is composed of well-separated peaks on a smooth background [Fig. 1(b) and 1(c)] [15].

Recently, self-pulsing was predicted in another physical context [11], and experimental confirmation came from microwave scattering in 2D resonators [12]. There the scattering echoes revealed a characteristic frequency of the internal weakly chaotic dynamics. No similar explanation applies to our (integrable) model. Another striking difference is the fact that in our case the delay-time density actually diverges at some of the peaks [Fig. 1(d)].

Our numerical results are reminiscent of transverse magnetic focusing [2], where the conductance between two point contacts to a 2DEG oscillates as a function of the magnetic field (or some other parameter) and shows a regular pattern of singularities [16]. The fundamental dynamical origin of these singularities are caustics of the classical electron motion. They correspond to the stationary points of a function that maps the incident angle to the exit location for an electron beam. Similarly we will explain the self-pulsing by *stationary points of the delay time* in the asymptotic phase space of scattering trajectories. To our knowledge, the effect of such stationary points has never been analyzed before, not in any kind of scattering system. Therefore, our results might be of interest beyond the study of electrons in a magnetic field, just as caustics in configuration space are relevant beyond magnetic focusing and in many different physical systems [17]. We shall come back to this point at the end of the Letter.

We consider electrons entering the channel of Fig. 1(a) from the left and with a given Fermi energy  $E_F = (m/2)v_F^2$ . Otherwise, the initial conditions  $0 \leq y \leq 1$  and  $|\varphi| \leq +\pi/2$  are randomly drawn from the microcanonical distribution restricted to  $x = 0$ ,  $p(y, \varphi) = \frac{1}{2} \cos \varphi$ . We use the channel width and the Fermi velocity as units of length and velocity, respectively ( $v_F = b = 1$ ). The cyclotron radius  $r = mv_F/eB$  and the length  $L$  of the system are free parameters [18]. Any trajectory is composed of circular arcs which are traversed clockwise (by convention about the direction of the magnetic field). For a point  $(x, y, \varphi)$  in phase space, the center of the current arc is the point  $(x_c, y_c) = (x + r \sin \varphi, y - r \cos \varphi)$ . Upon reflection from the channel walls  $y_c$  is conserved. Thus the system is integrable. We restrict attention to  $y_c < 0$ . For these trajectories the  $x$  component of the velocity is positive at any moment of time, and they generate the bulk of the left-to-right transmission delay distribution (up to  $t \sim 1270$  for the parameters of Fig. 1). We change variables to  $(\xi, \phi)$ , where  $0 \leq \phi = \arccos(-y_c/r) \leq \pi/2$  is the direction of the trajectory immediately after a reflection from the lower wall. In terms of this angle, the average transport velocity of a trajectory in an infinite channel is  $\bar{v}_x = \Delta x(\phi)/\Delta t(\phi)$ . Here

$$\Delta x(\phi) = 2r(\sin \phi - \sin \Phi), \quad (1)$$

$$\Delta t(\phi) = 2r(\phi - \Phi) \quad (2)$$

are the horizontal and the total length of the trajectory segment between two reflections from the lower wall, respectively. If  $\cos \phi \leq 1 - 1/r$ , the trajectory reaches the upper wall and is reflected there with the angle  $\Phi = \arccos(\cos \phi + \frac{1}{r})$  [see Fig. 1(a)].  $\Phi$  is set to zero for trajectories skipping along the lower wall only.  $\xi$  is the longitudinal location of the first reflection from the lower wall. We make the convention  $-\Delta x(\phi)/2 \leq \xi < \Delta x(\phi)/2$  such that negative values of  $\xi$  correspond to positive  $\varphi$  and vice versa. Explicitly, the transformation between  $(\varphi, y)$  and  $(\phi, \xi)$  is given by

$$y = r(\cos \varphi - \cos \phi), \quad (3)$$

$$-2\xi = 2r(\sin \phi - \sin \varphi) \quad (\xi < 0), \quad (4)$$

$$+2\xi = 2r(\sin \phi + \sin \varphi) \quad (\xi > 0). \quad (5)$$

The probability density in the new variables is  $p(\phi, \xi) = \frac{1}{2} \sin \phi$ .

As a first approximation to the delay time we ignore the dependence on  $\xi$  and set

$$\bar{\tau}(\phi) = \frac{L}{\bar{v}_x} = L \frac{\Delta t(\phi)}{\Delta x(\phi)}. \quad (6)$$

This results in the distribution

$$\bar{P}(t) = \int d\phi d\xi p(\phi, \xi) \delta(t - \bar{\tau}(\phi)) = \frac{\sin \phi_t \Delta x(\phi_t)}{2|\bar{\tau}'(\phi_t)|}, \quad (7)$$

where  $\phi_t$  is the root of  $\bar{\tau}(\phi) = t$ . For orbits which do not reach the upper wall we find

$$\bar{\tau}'(\phi) = L \frac{\sin \phi - \phi \cos \phi}{\sin^2 \phi} \quad (\cos \phi > 1 - r^{-1}), \quad (8)$$

$$\bar{P}(t) = \frac{r}{L} \frac{\sin^4 \phi_t}{\sin \phi_t - \phi_t \cos \phi_t} \quad (L < t < t^*). \quad (9)$$

Clearly, the transmission delay is bounded from below by  $t = L$  ( $\phi \rightarrow 0$ ). On the other hand,

$$t^*(L, r) = L \frac{\arccos(1 - r^{-1})}{\sqrt{2r^{-1} - r^{-2}}} \quad (10)$$

is the maximum delay for skipping orbits. Their contribution to  $\bar{P}(t)$  abruptly drops to zero at this point [ $t^* \approx 218.5$  in Fig. 1(b)]. Higher values  $t > t^*$  correspond to trajectories which bounce off both, the lower and the upper wall of the channel. We omit here the lengthy expression replacing Eq. (8) in this case. After substitution into Eq. (7) it yields the averaged delay-time distribution for  $t > t^*$  which is displayed together with Eq. (9) by the dashed white line in Fig. 1(b).

Now we come to the conspicuous oscillations in the delay-time density around its average value [Fig. 1(c)]. In general, the delay time  $\tau(\phi, \xi)$  depends on both variables,  $\phi$  and  $\xi$ . A variation of  $\xi$  corresponds to a longitudinal

shift of the trajectory [Fig. 1(a)] and results in [19]

$$\partial_\xi \tau(\phi, \xi) = (\cos\varphi)^{-1} - (\cos\varphi')^{-1}, \quad (11)$$

where  $\varphi$  and  $\varphi'$  are the inclination angles of the trajectory on entry and exit, respectively. However, if the length of the system is an integer multiple of the length of a segment,

$$L = n\Delta x(\phi_n), \quad (12)$$

these angles are equal. Only in this case the dependence of the delay time on  $\xi$  disappears and we have

$$\tau(\phi_n, \xi) = \bar{\tau}(\phi_n) = n\Delta t(\phi_n). \quad (13)$$

For each  $n$  there can be at most two solutions to Eq. (12), one corresponding to a skipping orbit and the other one not. We denote the corresponding delay times by  $t_n < t^*$  ( $n_{\min} \leq n$ ) and  $t'_n > t^*$  ( $n'_{\min} \leq n$ ), respectively. In Fig. 1(c) these values are marked with dashed vertical lines, and we see that they coincide with the peaks in the delay-time distribution. It is tempting to explain this observation by the following simple (and misleading) argument: typically, for a given  $\phi$  the various values of  $\xi$  contribute at different times to the density, while all of them add up in the same bin when  $\phi = \phi_n$ . So it is clear that the count should have a peak there. However, this cannot explain why the peaks at  $t_n$  are singularities of the density while the  $t'_n$  are finite maxima. To highlight this fact numerically we have magnified in Fig. 1(d) the density in the vicinity of  $t_{40}$  and observe that it grows as  $P(t) \propto \ln(t - t_n)$ . In contrast, the corresponding plot for  $t'_{40}$  [Fig. 1(e)] saturates to a finite value.

In order to understand the nature of the maxima we construct the function  $\tau(\phi, \xi)$  explicitly and represent the delay-time density as

$$\begin{aligned} P(t) &= \int d\phi \int d\xi p(\phi, \xi) \delta(t - \tau(\phi, \xi)) \\ &= \int d\xi \frac{p(\phi, \xi)}{|\partial_\phi \tau|} \Big|_{\phi=\phi(t, \xi)}. \end{aligned} \quad (14)$$

To this end, we decompose a trajectory into a number  $n$  of complete arcs and two additional terms for entry and exit. Formally we define  $n(\phi)$  as the best integer approximation to  $L/\Delta x$ , e.g.,  $n = 3$  in Fig. 1(a). The mismatch to exact commensurability will be denoted by

$$\delta L(\phi) = n\Delta x(\phi) - L. \quad (15)$$

According to Fig. 1(a) the delay time is given by

$$\tau(\phi, \xi) = n\Delta t(\phi) + s(\phi, \xi) - s(\phi, \xi') \quad (16)$$

with  $\xi' = \xi + \delta L(\phi)$ . In Eq. (16),  $s(\phi, \xi)$  is the length of the incomplete arc segment at the beginning of the trajectory. For  $\xi$  in Fig. 1(a) this is

$$\begin{aligned} s(\phi, \xi) &= r(\phi + \varphi) \quad (\varphi < 0, 0 \leq \xi \leq \Delta x(\phi)/2) \\ &= r[\phi + \arcsin(\xi/r - \sin\phi)] \end{aligned} \quad (17)$$

[the second line follows from Eq. (5)]. However,  $\xi'$  can

take values in the interval  $[-\Delta x(\phi), \Delta x(\phi)]$  since we have  $|\delta L(\phi)| < \frac{\Delta x}{2}$  and  $|\xi| < \frac{\Delta x}{2}$ . Therefore, we extend the domain of  $s(\phi, \xi)$  by the definitions

$$s(\phi, -\xi) = -s(\phi, \xi), \quad (18)$$

$$s(\phi, \Delta x(\phi) - \xi) = \Delta t(\phi) - s(\phi, \xi). \quad (19)$$

Note that  $s(\phi, \xi)$  is continuous at  $s(\phi, 0) = 0$  and  $s(\phi, \Delta x(\phi)/2) = \Delta t(\phi)/2$  but not analytic at  $\xi = 0$ . Equations (16)–(19) represent the delay time for  $0 \leq \phi \leq \frac{\pi}{2}$  and arbitrary values  $-\frac{\Delta x}{2} < \xi < +\frac{\Delta x}{2}$ . Figure 2 displays this function in the regions (a)  $t_{41} \leq t \leq t_{39}$  and (b)  $t'_{39} \leq t \leq t'_{41}$ . All level sets of constant delay time are one-dimensional curves in the two-dimensional phase space. In this respect there is nothing special about  $t = t_n$ , and thus the commensurability between system and trajectory cannot explain the maxima in the density. Rather we observe in Fig. 2(c)  $\partial_\phi \tau(\phi_n, 0) = 0$ . This is not immediately obvious from geometrical considerations but it can be confirmed analytically. We conclude that  $(\phi, \xi) = (\phi_n, 0)$  are *stationary points* of the delay time, and this is what really singles out the values  $t = t_n$ . No stationary points exist for  $t > t^*$  [Fig. 2(d)], although  $\partial_\phi \tau$  is very small close to  $\xi = \pm \Delta x(\phi)/2$ .

In the vicinity of the stationary points we can expand the delay time to second order,

$$\delta t = \frac{1}{2} \partial_{\phi\phi}^2 \tau \delta^2 \phi + \partial_{\phi\xi}^2 \tau \xi \delta \phi + \frac{1}{2} \partial_{\xi\xi}^2 \tau \xi^2, \quad (20)$$

solve for  $\delta\phi = \phi - \phi_n$ , and substitute the result into

$$\partial_\phi \tau = \partial_{\phi\phi}^2 \tau \delta\phi + \partial_{\phi\xi}^2 \tau \xi. \quad (21)$$

This gives  $\partial_\phi \tau$  as a function of  $\xi$  and  $\delta t = t - t_n$  and can be used in Eq. (14) to calculate the divergent contribution to the delay-time density. Unfortunately this procedure is more complicated than it may seem on first sight. Because of Eq. (18) we must distinguish for  $\delta t, \delta L > 0$  three regions (i)  $\xi > 0$ , (ii)  $\xi_0 < \xi < 0$ , and (iii)  $\xi < \xi_0$  (and

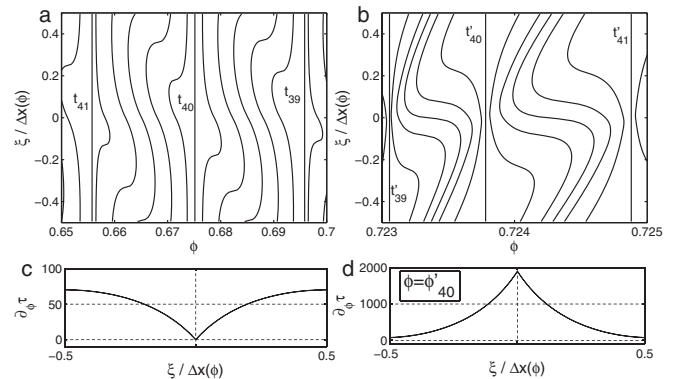


FIG. 2. Lines of constant delay time  $\tau(\xi, \phi) = t$  are shown in the vicinity of (a)  $t_{40}$  and (b)  $t'_{40}$ . The function  $\partial_\phi \tau$  vanishes at  $\phi = \phi_n$  and  $\xi = 0$  (c) while no stationary point exists for  $\phi = \phi'_n$  (d).

again three regions for  $\delta t$ ,  $\delta L < 0$ ). Here  $\xi_0(\delta t)$  is the point where the third term in Eq. (16) changes sign. It is given implicitly by the condition  $\xi_0 = -\delta L(\phi_n + \delta\phi)$ , where  $\delta\phi(\xi_0, \delta t)$  is the root of Eq. (20). Solving for  $\xi_0$  we find

$$\xi_0 = -(\sin\phi_n)^{-1}\sqrt{2\delta t(\cos^3\phi_n)/(2n-1)}. \quad (22)$$

Note that we did not drop the third term in Eq. (20). In fact, we have  $\partial_{\xi\xi}^2\tau \neq 0$  in the second region although  $\tau(\phi_n, \xi)$  is constant as a function of  $\xi$ . This is no contradiction since, according to Eq. (22), this region shrinks to a point for  $\phi = \phi_n$  [and hence is not visible in Fig. 2(d)]. With Eqs. (20)–(22) it can be shown that the contribution of region (ii) approaches a constant as  $\delta t \rightarrow 0$ . So it is irrelevant for our purpose. In the regions (i), (iii) we use  $\partial_{\xi\xi}^2\tau = 0$  and find

$$\partial_\phi\tau(\xi, \delta t) = \sqrt{(\partial_{\phi\xi}^2\tau)^2\xi^2 + 2\delta t\partial_{\phi\phi}^2\tau}, \quad (23)$$

$$\int \frac{d\xi}{|\partial_\phi\tau|} = \frac{1}{|\partial_{\phi\xi}^2\tau|} \ln(|\partial_{\phi\xi}^2\tau|\xi + |\partial_\phi\tau|) + \text{const.} \quad (24)$$

In region (i) the integral extends from  $\xi = 0$  to a value  $\sim \Delta x(\phi_n)/2$ . Its leading contribution is the logarithmic term  $|\ln\delta t/2\partial_{\phi\xi}^2\tau|$  from  $\xi = 0$ . The same contribution results from the upper limit  $\xi_0$  of region (iii), and in either case we have  $|\partial_{\phi\xi}^2\tau| = (L/r)(\cos\phi_n)^{-2}$ . Thus, together with the prefactor  $\frac{1}{2}\sin\phi_n = L/4nr$  from Eq. (14), we get

$$P(t) = \frac{1 - (L/2nr)^2}{4n} |\ln(t - t_n)| \quad (t \rightarrow t_n). \quad (25)$$

This prediction for the strength of the divergence has been confirmed numerically. For example both, a fit to the data in Fig. 1(d) and Eq. (25) yield a prefactor 0.00381 for  $n = 40$ .

The rather complicated analytical structure in the vicinity of the stationary points of the delay time and also the self-pulsing due to their regular arrangement are specific to our model. We would like to stress, however, that these features are not at all necessary for the appearance of singularities in the delay-time density. Generic stationary points for 2D scattering problems are extrema and saddle points. It is easy to see that saddle points lead again to a logarithmic divergence, while the density is finite at isolated maxima and minima. Although a logarithm is a rather weak singularity, it should lead to a prominent maximum in a histogram with finite resolution such as Fig. 1(c). This might be important, e.g., for inverse scattering problems. Consider, for example, a situation where it is difficult to control the precise initial conditions of test particles while their time delay can be measured with high precision. Then saddle points of the delay time will be among the dynamical

features which are directly accessible from experimental data. Therefore, it seems worthwhile to study them in more generic situations and independent of self-pulsing effects.

\*Electronic address: holger@nld.ds.mpg.de

- [1] C. M. Marcus *et al.*, Phys. Rev. Lett. **69**, 506 (1992); P. B. Wilkinson *et al.*, Nature (London) **380**, 608 (1996); A. S. Sachrajda *et al.*, Phys. Rev. Lett. **80**, 1948 (1998); A. P. S. de Moura *et al.*, Phys. Rev. Lett. **88**, 236804 (2002).
- [2] H. van Houten *et al.*, Phys. Rev. B **39**, 8556 (1989).
- [3] D. Weiss *et al.*, Phys. Rev. Lett. **66**, 2790 (1991); R. Fleischmann, T. Geisel, and R. Ketzmerick, Phys. Rev. Lett. **68**, 1367 (1992).
- [4] T. M. Fromhold *et al.*, Phys. Rev. Lett. **87**, 046803 (2001).
- [5] V. J. Goldman, B. Su, and J. K. Jain, Phys. Rev. Lett. **72**, 2065 (1994).
- [6] L. P. Rokhinson *et al.*, Phys. Rev. Lett. **93**, 146601 (2004).
- [7] E. P. Wigner, Phys. Rev. **98**, 145 (1955).
- [8] C. A. A. de Carvalho and H. M. Nussenzveig, Phys. Rep. **364**, 83 (2002).
- [9] Y. V. Fyodorov and H. J. Sommers, J. Math. Phys. (N.Y.) **38**, 1918 (1997).
- [10] A. Z. Genack *et al.*, Phys. Rev. Lett. **82**, 715 (1999); B. A. van Tiggelen, P. Sebbah, M. Stoytchev, and A. Z. Genack, Phys. Rev. E **59**, 7166 (1999).
- [11] C. Jung, C. Mejia-Monasterio, and T. H. Seligman, Europhys. Lett. **55**, 616 (2001); C. Jung *et al.*, New J. Phys. **6**, 48 (2004); H. Lee, C. Jung, and L. E. Reichl, Phys. Rev. B **73**, 195315 (2006).
- [12] C. Dembowski *et al.*, Phys. Rev. Lett. **93**, 134102 (2004).
- [13] E. A. Shaner and S. A. Lyon, Phys. Rev. Lett. **93**, 037402 (2004).
- [14] A. Yacoby *et al.*, Phys. Rev. Lett. **74**, 4047 (1995); R. Schuster *et al.*, Nature (London) **385**, 417 (1997); M. Sigrist *et al.*, Phys. Rev. Lett. **93**, 066802 (2004).
- [15] This is not the case in the absence of a magnetic field ( $r = \infty$ ). There the distribution is monotonically decreasing,  $P(t) = L^{-1}(L/t)^3(1 - [L/t]^2)^{-1/2}$  for  $t > L$ .
- [16] In reality these singularities are blurred by the finite contact width or by quantum effects [2]. An analogous smoothing of the delay-time singularities must be expected, but this will not be considered here.
- [17] F. Wright, Nature (London) **319**, 720 (1986); M. V. Berry and A. N. Wilson, Appl. Opt. **33**, 4714 (1994); M. A. Topinka *et al.*, Nature (London) **410**, 183 (2001); L. Kaplan, Phys. Rev. Lett. **89**, 184103 (2002); M. Wilkinson, B. Mehlig, and V. Bezuglyy, Phys. Rev. Lett. **97**, 048501 (2006).
- [18] Our results are not sensitive to the precise values of  $L$  and  $r$  as long as the magnetic field has a moderate strength  $r \geq 1$ . For numerical calculations we choose  $r = 4$  and  $L = 200$ .
- [19] We use a notation where, e.g.,  $\partial_\xi\tau$  stands for  $\partial\tau/\partial\xi$ . All second-order derivatives are evaluated at the stationary point  $(\phi, \xi) = (\phi_n, 0)$ .